Constraining the mixing matrix for the standard model with four generations: Time-dependent and semileptonic CP asymmetries in B_d^0, B_s, and D^0

Soumitra Nandi[1] and Amarjit Soni[2]

[1]*Physique des Particules, Université de Montréal, C.P. 6128, succ. centre-ville, Montréal, QC, Canada H3C 3J7*
[2]*Physics Department, Brookhaven National Laboratory, Upton, New York 11973, USA*

(Received 21 December 2010; published 16 June 2011)

Using existing experimental information from K, B, and D decays as well as electroweak precision tests and oblique parameters, we provide constraints and correlations on the parameters of the 4×4 mixing matrix for the standard model (SM) with four generations (SM4). We emphasize that some correlations amongst the parameters have important repercussions for key observables. We work with a particular representation of this matrix which is highly suited for extracting information from B decays. In particular, in our parametrization for SM4, we extend the hierarchical structure seen in SM with three generations as an expansion in powers of λ, the sine of the Cabbibo angle. Implications of the resulting constraints for time-dependent and semileptonic CP asymmetries for D^0, B^0, and for B_s are also given. While we show that the semileptonic asymmetries may be significantly enhanced in SM4 over the SM, there are important constraints and correlations with other observables. In particular, we find that despite significant enhancement in the semileptonic asymmetry $a_{\rm sl}^s$ for B_s over the SM, it is very difficult for SM4 to account for the central value of the recent D0 result, though given the large experimental error and other considerations, we do not regard this as a problem for SM4. Regarding the gold-plated measurement of $\sin 2\beta$ via $S_{\psi K_s}$, while SM4 can remove the tension that SM shows, as a consequence of one of the important correlations we find that the semileptonic asymmetry $a_{\rm sl}^d$ for B_d gets appreciably restricted in SM4. In this context we suggest that existing data from B factories taken on $\Upsilon(4S)$ and $\Upsilon(5S)$, and in the relevant continuum be used to constrain the semileptonic asymmetries for B_d, B_s as well as their linear combination. Of course, the data from the Tevatron and LHCb experiments can provide nontrivial tests of SM4 as well.

DOI: 10.1103/PhysRevD.83.114510 PACS numbers: 14.40.Nd, 13.20.Eb, 14.65.Jk

I. INTRODUCTION

In the past few years a number of tensions in the Cabibbo-Kobayashi-Maskawa (CKM) fits for the standard model (SM) with 3 generations (SM3) have been revealed [1–5]. There are quite serious indications that the "predicted" value of $\sin 2\beta$ is larger compared to the value measured directly via the "gold-plated" ψK_S mode by as much as $\approx 3.3\sigma$ [6]. Of course, the value of $\sin 2\beta$ determined from the penguin dominated modes tends to be even smaller compared to that from the ψK_s mode and therefore that constitutes even a larger deviation from the SM predicted value [2]. There are other anomalies as well that appear related. The difference in the partial rate asymmetries between $B^0 \to K^+\pi^-$ and $B^+ \to K^+\pi^0$ is also too large [7] to understand [2], though QCD complications do not allow us to draw compelling conclusions in this regard [8]. But with the backdrop of the hint of presence of a new CP-odd phase in the $\Delta S = 1$ penguin dominated modes, it is highly suggestive that the direct CP problem in $K\ \pi$ modes is receiving, at least in part, contribution from the same new physics (NP) source.

There are also some indications from the CDF and D0 experiments at the Tevatron [9]. While the earlier indication of possible nonstandard effects in $B_s \to \psi\phi$ seem to have weakened somewhat at the higher luminosity around $6/\text{fb}$ now being used [10], D0 has announced a surprisingly large CP asymmetry in the same sign dimuons which they attribute primarily to originate from $B_s \to X_s\mu\nu$ [11,12]. From a theoretical standpoint if new physics exists in $\Delta S = 1$ B decays, then it becomes highly unnatural for it not to exist in $\Delta S = 2$, B_s mixings as well.

A simple extension of the SM with four generations (SM4) can readily account for such anomalies [13–18]. Of course, even without these anomalies, SM4 is an interesting extension of the SM worth studying. The two extra phases that it possesses can give rise to a host of nonstandard CP asymmetries and in fact SM4 can significantly ameliorate the difficulties with regard to baryogenesis that SM3 has [19,20]. Besides, the heavier quarks and leptons of the 4th generation may well lead to dynamical electroweak symmetry breaking and thereby become useful in addressing the hierarchy problem without the need for supersymmetry at the weak scale [21–25]. Motivated by these considerations we will continue our investigations of the physical implications of SM4. In particular we will use all the known experimental constraints such as $B \to X_s\gamma$, $B \to X_s l^+ l^-$, ΔM_{B_s}, ΔM_{B_d}, $K^+ \to \pi\nu\nu$, $|\epsilon_k|$, and electroweak precision constraints from $Z \to b\bar{b}$ as well as oblique corrections [26,27] as in our previous work [13,14]. However, we will now use an explicit representation of the 4×4 CKM matrix of [28] given long ago. Although our basic idea to keep the elements of the fourth row as simple as possible is the same as in [28], we are extending the hierarchical structure of SM3 [29] to SM4 in our parameterization. We make this particular choice as it is very well designed to extract constraints from B decays since it was shown in a series of papers [28,30,31] that SM4 is highly susceptible to those decays. While physical results should not depend on the parameterization used, we believe in practice this representation would lead to a better determination of the underlying SM4 parameters.

We will provide constraints and many correlations amongst the 6 real parameters and the 3 phases that enter the SM4. We will then apply this framework to study mixing induced CP asymmetries $S(B_d \to \psi K_s)$, $S(B_s \to \psi \phi)$, $S(D^0 \to f)$ (where f may be any self conjugate final state such as $K_s\pi^0$, $K_s\omega$, $K_s\rho^0$, $\pi^0\pi^0$, K^+K^-, $\pi^+\pi^-$, etc.) and semileptonic asymmetries in D^0, B^0, and in B_s.

In obtaining these constraints and implications we will allow $m_{t'}$ to range from 375 to 575 GeV as suggested by current hints from study of B decays [13,14]. An interesting aspect of SM4 is that it is rather well constrained already. Thus, for example, while the semileptonic asymmetry in B_s ($a^s_{\rm sl}$) can be enhanced by as much as a factor of few hundreds over SM3 it still cannot account for the central value of the recent D0 result [11].[1] Of course, that observation has only about 2-σ significance and therefore rather large errors but improved experimental results could certainly rule out or confirm SM4, since the predicted range[2] in SM4 for $a^s_{\rm sl}$ is between about (-0.005) to (0.005). Note also that in SM4 a sign of $a^s_{\rm sl}$ has to be the same as $S_{\psi\phi}$. Furthermore, for B_d, $a^d_{\rm sl}$ can only be larger by around a factor of 3 over SM3. These semileptonic asymmetries also have interesting correlations with $S(B_s \to \psi\phi)$ and $S(B_d \to \psi K_s)$ respectively that should be testable.

As mentioned above one key difficulty for the CKM paradigm of SM3 uncovered in recent years is that the predicted value of $\sin 2\beta$ is too large compared to the measured one [1,6]. We will show here that SM4 tends to alleviate this tension appreciably but at the same time then it allows us to place an important bound on $a^d_{\rm sl}$ through the correlation mentioned in the previous paragraph.

B factories placed a bound on $a^d_{\rm sl}$ [10] some years ago but by now they have considerable more data. So an improved bound would be extremely worthwhile. In the past couple of years BELLE also took substantial data on $\Upsilon\,5S$ [33]. In fact that data could provide a very clean study of $a^s_{\rm sl}$ as well as on $A^b_{\rm sl}$, which is defined as the linear combination of $a^s_{\rm sl}$ and $a^d_{\rm sl}$ [12], since that sample provides a valuable source of this combination as well as an enriched sample of B_s. CDF, D0, and LHCb should be able to provide very useful results on these semileptonic asymmetries. In fact, whereas the Tevatron $p\bar{p}$ collider allowed D0 to yield the sum of $a^d_{\rm sl}$ and $a^s_{\rm sl}$, with the pp collider at LHC, the LHCb Collaboration plans to study the difference of these two asymmetries [34].

We should emphasize that in this series of studies on the 4th generation [13,14], for simplicity, and for definiteness, we have been making a tacit assumption that a heavy charge $2/3$ and $-1/3$ quark doublet has weak interaction just like the previous three families allowing us to incorporate these readily into a 4×4 mixing matrix resulting from an immediate generalization of the 3×3 case. Clearly if and when such a doublet of quarks is observed we will need to make detail tests on the weak interaction properties of the new quarks to verify that this assumption is correct.

The paper is arranged as follows. After the Introduction, in Sec. II A and II B we provide information regarding the parametrization and the constraints on the 4×4 CKM matrix by incorporating oblique corrections along with experimental data from important observables involving Z, B, and K decays as well as B_d and B_s mixings, etc. In Sec. II C, we present the estimates of many useful observables in the SM4. Finally, in Sec. III, we present our summary.

II. NUMERICAL ANALYSIS

A. Parametrization of $V_{\rm CKM4}$

We follow the idea of [28] in parametrizing the SM4 mixing matrix, then the elements of fourth row such as $V_{t'd}$, $V_{t's}$, and $V_{t'b}$, which are more relevant for the discussion of b physics, will be rather simple. However, our approach in parametrizing the elements of the SM4 mixing matrix is different from that one used in [28]. We parametrized the SM4 mixing matrix in terms of the nine parameters, λ, A, C, P, Q, r, δ_{ub}, $\delta_{t'd}$, and $\delta_{t's}$, by expanding each element of the matrix in powers of λ, the sine of the Cabbibo angle. In analogy with the Wolfenstein representation [29] for SM3 we assume a hierarchical structure for SM4 and define

$$V_{us} = \lambda, \qquad V_{cb} = A\lambda^2, \qquad V_{ub} = A\lambda^3 C e^{-i\delta_{ub}},$$
$$V_{t's} = -Q\lambda^2 e^{i\delta_{t's}}, \quad V_{t'd} = -P\lambda^3 e^{i\delta_{t'd}}, \quad V_{t'b} = -r\lambda, \qquad (1)$$

[1] Actually, the D0 experiment [11,12] reports a measurement of the linear combination, $A^b_{\rm sl}$, of the semileptonic asymmetry in B_d, $a^d_{\rm sl}$ and the one for B_s, $a^s_{\rm sl}$. They find $A^b_{sl} = (-0.957 \pm 0.251 \pm 0.146) \times 10^{-2}$ which is about 3.2σ away from the SM prediction, $A^b_{\rm sl}({\rm SM}) = (-2.3^{+0.5}_{-0.6}) \times 10^{-4}$ [32]. Using the existing upper bound from B factories [10], $a^d_{\rm sl} = -0.0047 \pm 0.0046$, D0 provides $a^s_{\rm sl} = -0.0146 \pm 0.0075$ which is just short of 2σ away from 0 and so also from the vanishingly small SM predicted value, $(2.1 \pm 0.6) \times 10^{-5}$ [32]. While the D0 result is extremely exciting it is a very challenging experiment, in particular, because the B mesons are not being identified or tagged. It is clearly extremely important to confirm their observation. For now we prefer to use the D0 results on these asymmetries with caution till confirmed and therefore we confine our comparison to their result on $a^s_{\rm sl}$, wherein it is considerably diluted due to their use of the B-factory bound on $a^d_{\rm sl}$.

[2] In arriving at this range, conservatively we have enlarged the theory error in $\frac{|\Gamma^s_{12}|}{|M^{s,{\rm SM}}_{12}|}$ to 2σ.

with the generalized 4×4 mixing-matrix V_{SM4} as given in Eq. (3). With the inputs $|V_{ub}| = (32.8 \pm 3.9) \times 10^{-4}$ and $|V_{cb}| = (40.86 \pm 1.0) \times 10^{-3}$ taken at 1σ, constraints obtained on A and C are given by

$$0.825 \le A \le 0.865, \qquad 0.32 \le C \le 0.42, \tag{2}$$

while $\lambda = 0.2205 \pm 0.0018$. The phase of V_{ub}, i.e., δ_{ub} can be taken as the CKM angle γ of SM3. We do not have sufficient data to exclude the ranges like $P < 1$, $Q < 1$ and $r < 1$, therefore we treat them as free parameters and then constrain them;

$$\begin{pmatrix} 1-\frac{\lambda^2}{2}+\mathcal{O}(\lambda^4) & \lambda & A\lambda^3 C e^{-i\delta_{ub}} & \begin{array}{c} P\lambda^3 e^{-i\delta_{t'd}} \\ +Q\lambda^3 e^{-i\delta_{t's}} + ACr\lambda^4 e^{-i\delta_{ub}} \\ -P\frac{\lambda^5}{2} e^{-i\delta_{t'd}} + \mathcal{O}(\lambda^7) \end{array} \\ -\lambda+\mathcal{O}(\lambda^5) & 1-\frac{\lambda^2}{2}+O(\lambda^4) & A\lambda^2 & \begin{array}{c} Q\lambda^2 e^{-i\delta_{t's}} \\ +A\lambda^3 r - P\lambda^4 e^{-i\delta_{t'd}} \\ -\frac{Q}{2}\lambda^4 e^{-i\delta_{t's}} + \mathcal{O}(\lambda^6) \end{array} \\ \begin{array}{c} A\lambda^3(1-Ce^{i\delta_{ub}}) \\ -Pr\lambda^4 e^{i\delta_{t'd}} \\ +\frac{1}{2}AC\lambda^5 e^{i\delta_{ub}} + \mathcal{O}(\lambda^7) \end{array} & \begin{array}{c} -A\lambda^2 - Qr\lambda^3 e^{i\delta_{t's}} \\ +A\lambda^4\left(\frac{1}{2} - Ce^{i\delta_{ub}}\right) \\ +\mathcal{O}(\lambda^6) \end{array} & 1-\frac{r^2\lambda^2}{2}+\mathcal{O}(\lambda^4) & r\lambda + \mathcal{O}(\lambda^4) \\ -P\lambda^3 e^{i\delta_{t'd}} & -Q\lambda^2 e^{i\delta_{t's}} & -r\lambda & 1-\frac{r^2\lambda^2}{2}+\mathcal{O}(\lambda^4) \end{pmatrix}. \tag{3}$$

B. Inputs

In our earlier papers [13,14], to find the limits on some of the V_{CKM4} elements, we concentrated mainly on the constraints that will come from nondecoupling oblique corrections, vertex correction to $Z \to b\bar{b}$, $\mathcal{BR}(B \to X_s\gamma)$, $\mathcal{BR}(B \to X_s l^+ l^-)$, $B_d - \bar{B}_d$, and $B_s - \bar{B}_s$ mixing, $\mathcal{BR}(K^+ \to \pi^+ \nu\nu)$ and the indirect CP violation in $K_L \to \pi\pi$ described by ϵ_k; we did not consider ϵ'/ϵ as a constraint because of the large hadronic uncertainties in the evaluation of its matrix elements. With the inputs given in Table I we have made the scan over the entire parameter space by a flat random number generator "RAN1(J)" where "J" is the number of iterations. As mentioned in the previous section we constrain the parameters A and C from the data on $|V_{cb}|$ and $|V_{ub}|$. $\Gamma(Z \to b\bar{b})$ and the nondecoupling oblique corrections such as T_4 are functions of $|V_{t'b}|^2$ and $|V_{tb}|^2$ or equivalently functions of r or higher powers of r, thus we get direct constraint on r from these data. All the other observables in Table I are functions of either $\lambda_{bs}^{t'} = V_{t'b}V_{t's}^*$ and $\lambda_{bs}^{t} = V_{tb}V_{ts}^*$ or $\lambda_{bd}^{t'} = V_{t'b}V_{t'd}^*$ and $\lambda_{bd}^{t} = V_{tb}V_{td}^*$ or both. Furthermore, we can use unitarity relation, like $\lambda_{bq}^{u} + \lambda_{bq}^{c} + \lambda_{bq}^{t} + \lambda_{bq}^{t'} = 0$ with

TABLE I. Inputs that we use in order to constrain the SM4 parameter space, when not explicitly stated, we take the inputs from Particle Data Group [7]; for the lattice inputs see also [6].

$B_K = 0.740 \pm 0.025$ [35–37]	$R_{bb} = 0.216 \pm 0.001$
$f_{bd}\sqrt{B_{bd}} = 0.224 \pm 0.015$ GeV [38,39]	$\|V_{ub}\| = (32.8 \pm 2.6) \times 10^{-4}$ [a]
$\xi = 1.232 \pm 0.042$ [38,39]	$\|V_{cb}\| = (40.86 \pm 1.0) \times 10^{-3}$
$\eta_c = 1.51 \pm 0.24$ [40]	$\gamma = (73.0 \pm 13.0)^\circ$
$\eta_t = 0.5765 \pm 0.0065$ [41]	$\mathcal{BR}(B \to X_s\gamma) = (3.55 \pm 0.25) \times 10^{-4}$
$\eta_{ct} = 0.494 \pm 0.046$ [42]	$\mathcal{BR}(B \to X_s \ell^+\ell^-) = (0.44 \pm 0.12) \times 10^{-6}$
$\Delta M_s = (17.77 \pm 0.12)\ \mathrm{ps}^{-1}$	$\mathcal{BR}(K^+ \to \pi^+\nu\nu) = (0.147^{+0.130}_{-0.089}) \times 10^{-9}$
$\Delta M_d = (0.507 \pm 0.005)\ \mathrm{ps}^{-1}$	$\mathcal{BR}(B \to X_c \ell\nu) = (10.61 \pm 0.17) \times 10^{-2}$
$\|\epsilon_k\| \times 10^3 = 2.32 \pm 0.007$	$T_4 = 0.11 \pm 0.14$
$\kappa_\epsilon = 0.94 \pm 0.02$ [43][b]	$m_t(m_t) = (163.5 \pm 1.7)$ GeV

[a]It is the weighted average of $V_{ub}^{\mathrm{inl}} = (40.1 \pm 2.7 \pm 4.0) \times 10^{-4}$ and $V_{ub}^{\mathrm{exl}} = (29.7 \pm 3.1) \times 10^{-4}$. In our numerical work to follow, we increase the error on $|V_{ub}|$ by 50% and take the total error to be around 12% because of the appreciable disagreement between the two determinations.
[b]We tacitly assume that κ_ϵ in SM4 is approximately the same as in SM3.

$q = d, s$, to reduce the number of independent elements, therefore, it is possible to constrain the magnitudes and phases of these elements directly from the data as we did in our previous studies [13,14]. However, in this paper, we express all these elements in terms of new SM4 parameters such as, P, Q, r, $\delta_{t'd}$, and $\delta_{t's}$ of the 4×4 mixing matrix, Eq. (3), or equivalently we express all the observables as functions of these parameters. We allow these parameters to vary randomly over a broad range and finally constrain them from the data. After satisfying all the constraints we get $\approx 8 \times 10^3$ data points in a multidimensional parameter space for $J = 2 \times 10^9$.

From direct searches at the Tevatron, it follows that $m_{t'} > 335$ GeV [44]. Taking into account the limits from electroweak precision tests [45–48], perturbativity [49], and indications from our studies [13,14], plausible ranges for $m_{t'}$ and $m_{b'}$ can be taken as

$$\begin{aligned} &375\ \text{GeV} < m_{t'} < 575\ \text{GeV}, \\ &m_{t'} - m_{b'} \approx \left(1 + \frac{1}{5}\ln\frac{m_H}{115\ \text{GeV}}\right) \times 55\ \text{GeV}. \end{aligned} \tag{4}$$

Here the mass splitting depends on the Higgs mass, however, for simplicity we do not consider the variation of Higgs mass and take mass splitting to be ≈ 50 GeV.

Detailed formulas for the above mentioned observables (Table I) can be seen from one of our earlier papers [14]. In this paper, we do not impose $S_{\psi K_s} = \sin 2\beta_{\text{eff}}$ as a constraint, we show a SM4 prediction for $S_{\psi K_s}$ and its correlation with the semileptonic asymmetry a^d_{sl}. The expression for the semileptonic asymmetry is given by

$$a^q_{\text{sl}} = \frac{|\Gamma^q_{12}|}{|M^q_{12}|}\sin\phi_q = \frac{|\Gamma^q_{12}|}{|M^{q,\text{SM}}_{12}|}\frac{\sin\phi_q}{|\Delta_q|}, \quad (q = d, s), \tag{5}$$

where $|\Gamma^q_{12}|$, $|M^q_{12}|$ are the width and mass differences between heavy and light mass eigenstates of B_q mesons, and the CP violating phase ϕ_q ($q = d$, s) is defined as

$$\phi_q \equiv \text{Arg}\left[-\frac{M^q_{12}}{\Gamma^q_{12}}\right]. \tag{6}$$

In Eq. (5), Δ_q parametrized the new physics effects in mixing and defined as

$$M^q_{12} = M^{q,\text{SM}}_{12}\left(1 + \frac{M^{q,\text{NP}}_{12}}{M^{q,\text{SM}}_{12}}\right) = M^{q,\text{SM}}_{12}\Delta_q. \tag{7}$$

In the SM the CP phases are small, $\phi_d \approx -4.3°$ and $\phi_s \approx 0.22°$ [32], new physics can affect the magnitude and phase of M^q_{12}, hence ΔM_q and ϕ_q can deviate substantially from their SM predictions. The semileptonic asymmetry is the function of the CP phase ϕ_q, $|\Delta_q|$ and the ratio $\frac{|\Gamma^q_{12}|}{|M^{q,\text{SM}}_{12}|}$ ($q = d$, s). The SM predictions for Γ^q_{12} suffer from large theoretical uncertainties which are $\approx 40\%$ and 30% for the B_s and B_d system, respectively, [32], however, in the ratio $\frac{|\Gamma^q_{12}|}{|M^{q,\text{SM}}_{12}|}$ hadronic uncertainties due to the decay constants f_{B_q} cancel to a large extent. In the B_d and B_s system one has [32]

$$\begin{aligned} \frac{|\Gamma^d_{12}|}{|M^{d,\text{SM}}_{12}|} &= (52.6^{+11.5}_{-12.8}) \times 10^{-4}, \\ \frac{|\Gamma^s_{12}|}{|M^{s,\text{SM}}_{12}|} &= (4.97 \pm 0.94) \times 10^{-3}, \end{aligned} \tag{8}$$

with the theoretical error in both the cases $\approx 20\%$. However, to predict a^q_{sl} in any NP scenario one needs to constrain $|\Delta_q|$ from the data on ΔM_q; Eq. (7), therefore, this gets limited by the precision of the lattice calculations.

We also study $D^0 - \bar{D}^0$ mixing in the presence of a fourth generation of quarks [16]. In particular, we calculate the size of the allowed CP violation, which could be large compared to the SM, and show its parametric dependence on CKM4 elements.

Within the SM, $D^0 - \bar{D}^0$ mixing proceeds to an excellent approximation only through the box diagrams with internal b and s quark exchanges. In the case of four generations there is an additional important contribution to $D^0 - \bar{D}^0$ mixing coming from the virtual exchange of the fourth generation down quark b'.

The short distance (SD) contributions to the matrix element of the $\Delta C = 2$ effective Hamiltonian can be written as

$$\langle \bar{D}^0 | \mathcal{H}^{\Delta C=2}_{\text{eff}} | D^0 \rangle_{\text{SD}} \equiv |M^D_{12}| e^{2i\phi_D} = (M^D_{12})^*, \tag{9}$$

where

$$M^D_{12} = \frac{G_F^2}{12\pi^2} f_D^2 \hat{B}_D m_D M_W^2 \bar{M}^D_{12}, \tag{10}$$

with

$$\begin{aligned} \bar{M}^D_{12} = {} & \lambda_s^{(D)*2}\eta^{(K)}_{cc} S_0(x_s) + \lambda_b^{(D)*2}\eta^{(K)}_{cc} S_0(x_b) \\ & + \lambda_{b'}^{(D)*2}\eta^{(K)}_{tt} S_0(x_{b'}) + 2\lambda_b^{(D)*}\lambda_s^{(D)*}\eta^{(K)}_{cc} S_0(x_b, x_s) \\ & + 2\lambda_{b'}^{(D)*}\lambda_s^{(D)*}\eta^{(K)}_{ct} S_0(x_{b'}, x_s) \\ & + 2\lambda_{b'}^{(D)*}\lambda_b^{(D)*}\eta^{(K)}_{ct} S_0(x_{b'}, x_b), \end{aligned} \tag{11}$$

where

$$\lambda_i^{(D)} = V^*_{ci} V_{ui} (i = s, b, b'). \tag{12}$$

For the QCD corrections we will use the approximate relations

$$\begin{aligned} &\eta^{(D)}_{b'b'} \approx \eta^{(K)}_{tt}, \\ &\eta^{(D)}_{b'b} \approx \eta^{(D)}_{b's} \approx \eta^{(K)}_{ct}, \\ &\eta^{(D)}_{ss} \approx \eta^{(D)}_{bb} \approx \eta^{(D)}_{bs} \approx \eta^{(K)}_{cc}. \end{aligned} \tag{13}$$

Including the long distance part the full matrix elements are given by

$$\langle \bar{D}^0 | \mathcal{H}^{\Delta C=2}_{\text{eff}} | D^0 \rangle = (M^D_{12} + M^{\text{LD}}_{12})^* - \frac{i}{2}\Gamma^{\text{LD}^*}_{12}, \tag{14}$$

TABLE II. Values of the input parameters for D mesons used in our analysis.

Parameter	Value	Parameter	Value
m_D	$(1.864\,84 \pm 0.000\,17)$ GeV	$\bar{\tau}_D$	(0.4101 ± 0.0015) ps
f_D	(0.212 ± 0.014) GeV [55]	$m_c(m_c)$	(1.268 ± 0.009) GeV [56,57]
$\hat{B}_D$	$1.18^{+0.07}_{-0.05}$ [16,58]	$m_b(m_b)$	$(4.20^{+0.17}_{-0.07})$ GeV [52]

$$\langle D^0|\mathcal{H}_{\rm eff}^{\Delta C=2}|\bar{D}^0\rangle = (M_{12}^D + M_{12}^{\rm LD}) - \frac{i}{2}\Gamma_{12}^{\rm LD}. \tag{15}$$

Here $\Gamma_{12}^{\rm LD}$ and $M_{12}^{\rm LD}$ stand for long distance (LD) contributions with the former arising exclusively from SM3 dynamics. These contributions are very difficult to estimate reliably. In our work we scan flatly over the intervals [50,51].

$$-0.02\ {\rm ps}^{-1} \le M_{12}^{\rm LD} \le 0.02\ {\rm ps}^{-1}, \tag{16}$$

$$-0.04\ {\rm ps}^{-1} \le \Gamma_{12}^{\rm LD} \le 0.04\ {\rm ps}^{-1}. \tag{17}$$

$D^0 - \bar{D}^0$ oscillations can be characterized by the normalized mass and width differences

$$x_D \equiv \frac{\Delta M_D}{\bar{\Gamma}}, \qquad y_D \equiv \frac{\Delta\Gamma_D}{2\bar{\Gamma}}, \qquad \bar{\Gamma} = \frac{1}{2}(\Gamma_1 + \Gamma_2), \tag{18}$$

with

$$\Delta M_D = M_1 - M_2 = 2\,{\rm Re}\left[\frac{q}{p}\left(M_{12}^D - \frac{i}{2}\Gamma_{12}^D\right)\right] = 2\,{\rm Re}\sqrt{|M_{12}^D|^2 - \frac{1}{4}|\Gamma_{12}^D|^2 - i\,{\rm Re}(\Gamma_{12}^D M_{12}^{D*})}, \tag{19}$$

$$\Delta\Gamma_D = \Gamma_1 - \Gamma_2 = -4\,{\rm Im}\left[\frac{q}{p}\left(M_{12}^D - \frac{i}{2}\Gamma_{12}^D\right)\right] = -4\,{\rm Im}\sqrt{|M_{12}^D|^2 - \frac{1}{4}|\Gamma_{12}^D|^2 - i\,{\rm Re}(\Gamma_{12}^D M_{12}^{D*})}, \tag{20}$$

where

$$\frac{q}{p} \equiv \sqrt{\frac{M_{12}^{D*} - \frac{i}{2}\Gamma_{12}^{D*}}{M_{12}^D - \frac{i}{2}\Gamma_{12}^D}}. \tag{21}$$

For practical purposes it is sufficient to consider the time-dependent CP asymmetry S_f as [50]

$$\frac{\Gamma(D^0(t)\to f) - \Gamma(\bar{D}^0(t)\to f)}{\Gamma(D^0(t)\to f) + \Gamma(\bar{D}^0(t)\to f)} \equiv S_f(D)\frac{t}{2\bar{\tau}_D}, \tag{22}$$

which is given by

$$\eta_f S_f(D) \simeq -\left[y_D\left(\left|\frac{q}{p}\right| - \left|\frac{p}{q}\right|\right)\cos\varphi - x_D\left(\left|\frac{q}{p}\right| + \left|\frac{p}{q}\right|\right)\sin\varphi\right], \tag{23}$$

where $\eta_f = \pm 1$ is the CP parity of the final state f. The SM3 prediction for $\eta_f S_f(D)$ is [16,50]

$$[\eta_f S_f(D)]_{\rm SM3} \approx -2\times 10^{-6}. \tag{24}$$

Finally, the semileptonic asymmetry is defined as

$$a_{\rm SL}(D) \equiv \frac{\Gamma(D^0(t)\to \ell^-\bar{\nu}K^{+(*)}) - \Gamma(\bar{D}^0\to \ell^+\nu K^{-(*)})}{\Gamma(D^0(t)\to \ell^-\bar{\nu}K^{+(*)}) + \Gamma(\bar{D}^0\to \ell^+\nu K^{-(*)})} = \frac{|q|^4 - |p|^4}{|q|^4 + |p|^4} \approx 2\left(\left|\frac{q}{p}\right| - 1\right). \tag{25}$$

The world averages based on data from *BABAR*, Belle, and CDF are given by [52–54]

$$x_D = (0.98^{+0.24}_{-0.26})\%, \qquad y_D = (0.83 \pm 0.16)\%,$$
$$|q/p| = (0.87^{+0.17}_{-0.15}), \qquad \phi = (-8.5^{+7.4}_{-7.0})^\circ,$$
$$\eta_f S_f(D) = (-0.248 \pm 0.496)\%, \tag{26}$$

with ϕ being the phase of q/p and the asymmetry $\eta_f S_f(D)$ defined in (22).

In addition to Table I the relevant input parameters for $D^0 - \bar{D}^0$ mixing are given in Table II.

C. Results

Allowed ranges for different CKM4 parameters are given in Table III. Constraint on $V_{t'b}$ or equivalently on the new parameter r (i.e. $V_{t'b} = -r\lambda$) is obtained from nondecoupling oblique corrections (T_4) and vertex corrections to $Z \to b\bar{b}$. We also note the allowed ranges for the product of the different CKM4 elements, $|\lambda_{db}^{t'}| = |V_{t'd}^* V_{t'b}|$, $|\lambda_{sb}^{t'}| = |V_{t's}^* V_{t'b}|$, and $|\lambda_{uc}^{b'}| = |V_{ub'}^* V_{cb'}|$, obtained from our analysis; these are relevant to B_d^0, B_s, and D^0 oscillations. Allowed ranges for the corresponding

TABLE III. Allowed ranges of the CKM4 parameters obtained from our analysis.

Parameter	Allowed range	Parameter	Allowed range
λ	0.2205 ± 0.0018	$\lvert V_{t'b}\rvert$	<0.12
C	$0.32 \to 0.42$	$\lvert V_{t'd}\rvert$	<0.05
A	$0.825 \to 0.865$	$\lvert V_{t's}\rvert$	<0.11
γ	$(73 \pm 13)^\circ$	$\lvert V_{ub'}\rvert$	<0.05
r	<0.5	$\lvert V_{cb'}\rvert$	<0.11
P	<5.0	$\lvert\lambda_{db}^{t'}\rvert$	<0.002
Q	<2.5	$\lvert\lambda_{sb}^{t'}\rvert$	<0.01
		$\lvert\lambda_{uc}^{b'}\rvert$	<0.0025

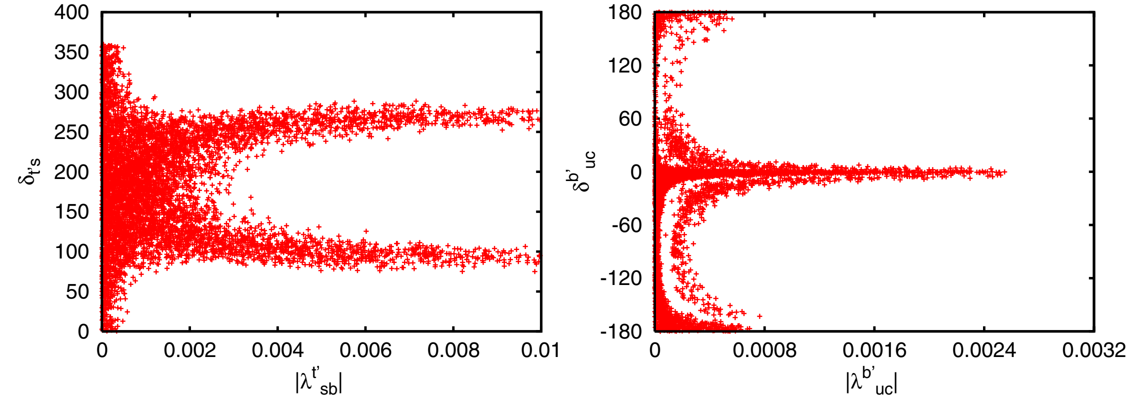

FIG. 1 (color online). Fourth generation parameter space; the left panel shows the variation of $|\lambda_{sb}^{t'}| = |V_{t's}^* V_{t'b}|$ with the phase $\delta_{t's}$ of $V_{t's}$, whereas the right panel shows it for $|\lambda_{uc}^{b'}| = |V_{ub'}^* V_{cb'}|$ with $\delta_{uc}^{b'}$, the phase difference between the phase of $V_{ub'}^*$ and $V_{cb'}$.

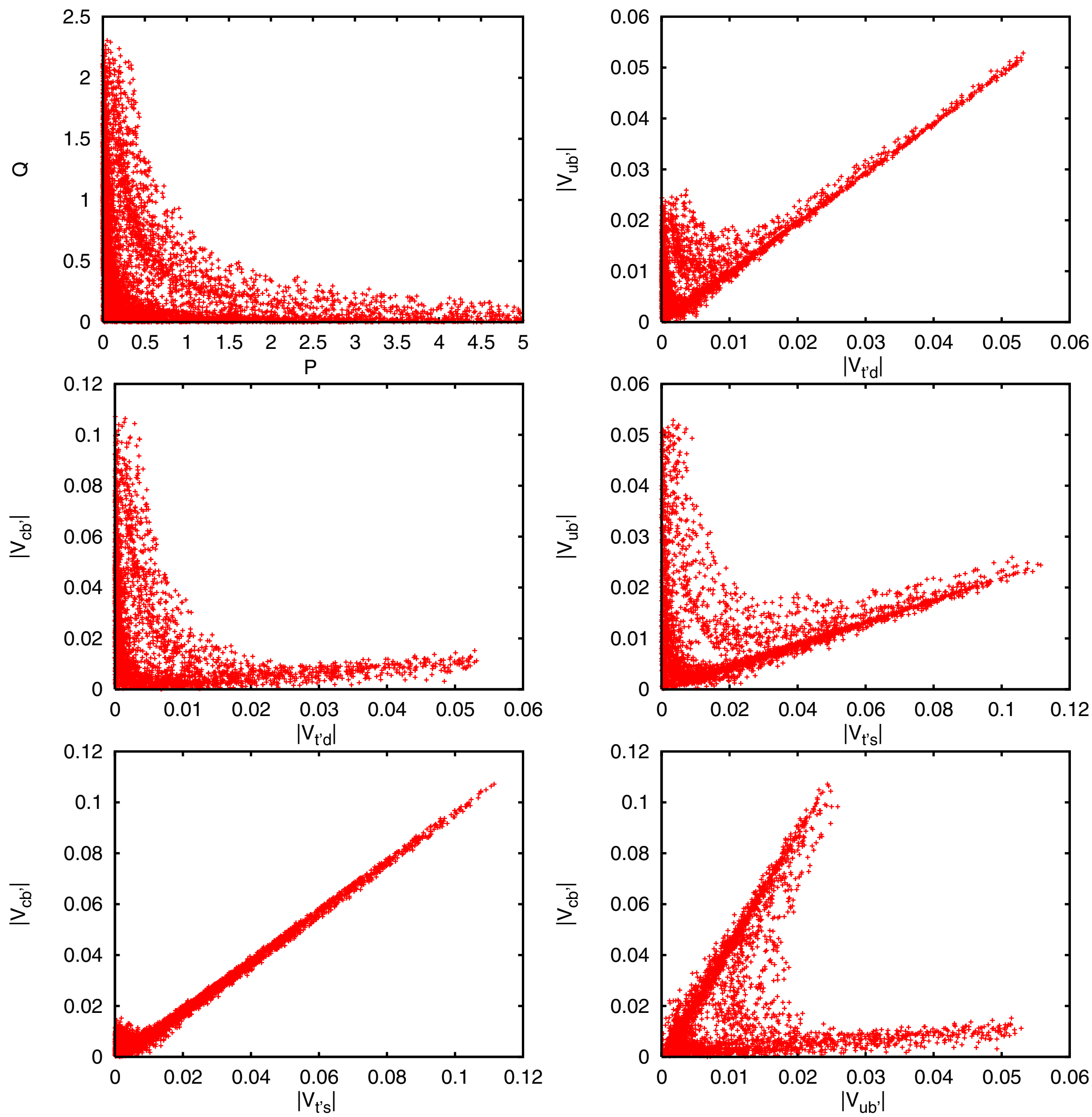

FIG. 2 (color online). Correlations between different new CKM4 elements are shown.

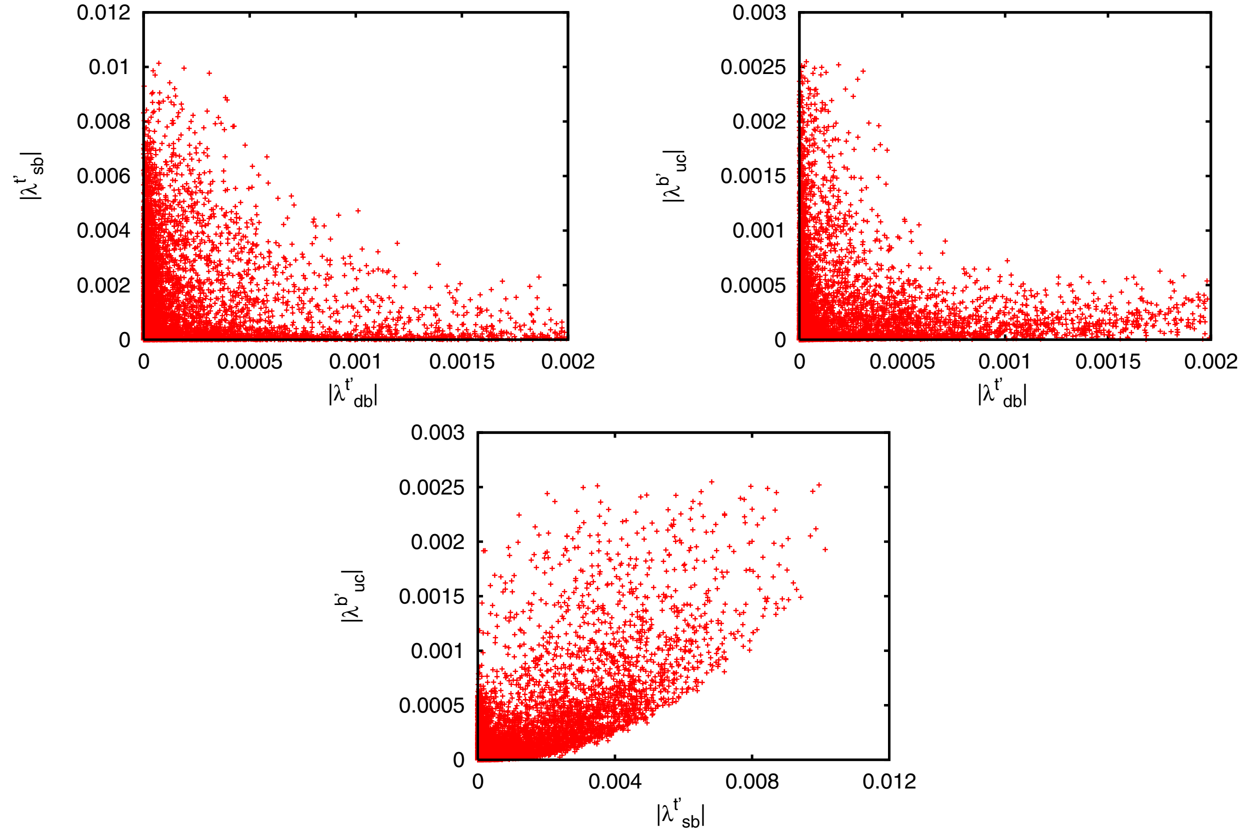

FIG. 3 (color online). Correlations between different CKM4 product couplings are shown: $|\lambda^{t'}_{db}| = |V^*_{t'd}V_{t'b}|$ and $|\lambda^{t'}_{sb}| = |V^*_{t's}V_{t'b}|$ (upper-left panel), $|\lambda^{t'}_{db}|$ and $|\lambda^{b'}_{uc}| = |V^*_{ub'}V_{cb'}|$ (upper-right panel), $|\lambda^{t'}_{sb}|$ and $|\lambda^{b'}_{uc}|$ (lower-panel).

phases and their correlations with the magnitude of the product couplings are shown in Fig. 1. We note that values of $|\lambda^{t'}_{sb}|$ larger than 0.002 correspond to very narrow regions of the phase $\delta_{t's}$ (left panel, Fig. 1) close to 90° or 270°, whereas that for $\delta^{b'}_{uc} = \delta_{cb'} - \delta_{ub'}$ (right panel) is close to zero when $|\lambda^{b'}_{uc}| \gtrsim 0.0008$. $B_d - \bar{B}_d$ and $B_s - \bar{B}_s$ mixing are sensitive to the new parameters $[P, \delta_{t'd}]$ and $[Q, \delta_{t's}]$, respectively, whereas $K^0 - \bar{K}^0$ and $D^0 - \bar{D}^0$ mixing are sensitive to all these four new parameters and their parametric dependencies are given by

$$\begin{aligned}\lambda^{t'}_{ds} &= V^*_{t's}V_{t'd} = PQ\lambda^5 e^{i(\delta_{t'd}-\delta_{t's})}\\ \lambda^{b'}_{uc} &= V^*_{ub'}V_{cb'} = Q\lambda^5(Q + Pe^{i(\delta_{t'd}-\delta_{t's})}),\end{aligned} \tag{27}$$

respectively. In this framework it is quite natural to expect that there is a strong correlation between $K^0 - \bar{K}^0$ and $D^0 - \bar{D}^0$ mixing, as pointed out in the case of purely left-handed currents [50,59], $D^0 - \bar{D}^0$ mixing is also correlated with the observables from B_d and B_s mixing and decays. So the constraints obtained on the new parameters from the inputs given in Table I, especially ϵ_K and $\mathrm{Br}(K^+ \to \pi^+\nu\bar{\nu})$, are helpful to find the allowed parameter space for $\lambda^{b'}_{uc}$ and the corresponding phase difference $\delta^{b'}_{uc}$.

In Fig. 2 (upper-left panel) we show the correlation between P and Q, larger values of P correspond to the lower value of Q and vice versa. We obtain such a correlation mainly due to the constraints from ϵ_K and $\mathrm{Br}(K^+ \to \pi^+\nu\bar{\nu})$, although the upper bound on P and Q is coming from the B_d and B_s data (see Table I). The expressions for ϵ_K and $\mathrm{Br}(K^+ \to \pi^+\nu\bar{\nu})$ are sensitive to $\lambda^{t'}_{ds}$, i.e., using these inputs we will get direct constraint on $\lambda^{t'}_{ds}$; as indicated in Eq. (27), $\lambda^{t'}_{ds}$ is proportional to the product of P and Q. Therefore, we will get direct constraint on the product not on individual P or Q and this is the reason why they follow the correlations shown. A similar correlation is possible between $V_{t'd}$ and $V_{t's}$ since they are proportional to P and Q, respectively. We also show the correlations between some other CKM4 elements [3]; the plot of $|V_{t's}|$ as a function of $|V_{cb'}|$ (lower-left panel) shows that $|V_{t's}| \approx |V_{cb'}|$ since leading order contribution to both the terms is proportional to Q. However, the plot of $|V_{t'd}|$ as a function of $|V_{ub'}|$ (upper-right panel) shows such a relationship only when $P \gg Q$ since the leading order contribution to $|V_{t'd}|$ is proportional to P whereas that for $|V_{ub'}|$

[3]Flavor data allows us to get direct constraints on various products of CKM4 elements. The bounds on individual CKM4 element are obtained using the constraints on the product couplings. Data for nondecoupling oblique corrections helps to get tighter constraints on $|V_{t'b}|$ which helps to constrain $|V_{t's/d}|$ from the bound on $|\lambda^{t'}_{s/db}|$.

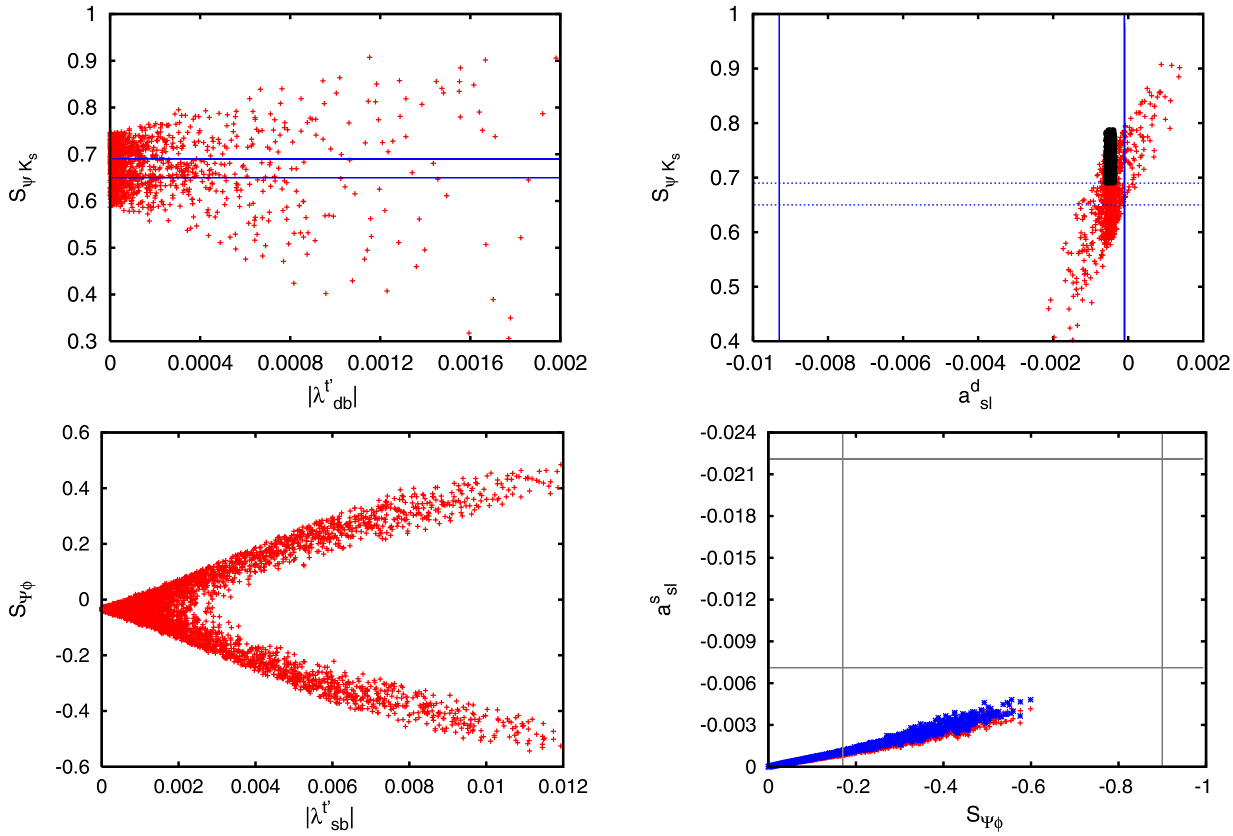

FIG. 4 (color online). Various correlations in SM4 are shown. Variation of CP asymmetries with the magnitude of the product couplings; $S_{\psi K_s}$ as a function of $|\lambda^{t'}_{db}|$ (upper-left panel), $S_{\psi\phi}$ as a function of $|\lambda^{t'}_{sb}|$ (lower-left panel). Correlations between the time-dependent mixing induced CP asymmetries and semileptonic CP asymmetries for B_d and B_s are shown in the upper and lower-right panels, respectively. Blue horizontal and vertical bands are the corresponding experimental ranges. In the upper-right panel the SM allowed band (thick dark) is shown in the $S_{\psi K_s}$ vs $a^d_{\rm sl}$ plane. In the lower-right panel the red and blue regions correspond to $\frac{|\Gamma^s_{12}|}{|M^{s,\rm SM}_{12}|}$ with the uncertainties taken at 1σ and 2σ, respectively, and the grey horizontal band corresponds to the experimental range for $a^s_{\rm sl}$ and the vertical band is that for CP asymmetry.

is proportional to a linear combination of P and Q, see Eq. (3). For relatively smaller values of $|V_{t'd}|$, of $\mathcal{O}(10^{-3})$, $|V_{ub'}|$ could be as high as 0.02; this is possible when $Q > P$ or alternatively when $|V_{t's}| \gtrsim 0.025$ (middle-right panel, Fig. 2). It also shows that larger values of $|V_{ub'}|$ are still possible which correspond to $P \gg Q$, i.e., for smaller values of $|V_{t's}|$. Similar feature can be observed in the correlation between $|V_{ub'}|$ and $|V_{cb'}|$ (lower-right panel). The middle-left panel of Fig. 2 shows the correlation between $|V_{t'd}|$ and $|V_{cb'}|$, which is similar to the correlation between P and Q since leading order contribution in $|V_{cb'}|$ is $\propto Q$ and that for $|V_{cb'}|$ is $\propto P$.

The expressions for the product of CKM4 elements $|\lambda^{t'}_{db}|$ and $|\lambda^{t'}_{sb}|$ are given by

$$|\lambda^{t'}_{db}| = |V^*_{t'd}V_{t'b}| = Pr\lambda^4,$$
$$|\lambda^{t'}_{sb}| = |V^*_{t's}V_{t'b}| = Qr\lambda^3, \qquad (28)$$

whereas that for $|\lambda^{b'}_{uc}|$ can be obtained from Eq. (27) by taking its modulus, and we see that when $P \ll Q$ it is $\approx Q^2\lambda^5$. In Fig. 3 we show the correlations between the products of CKM4 elements; the upper-left panel shows the correlation between $|\lambda^{t'}_{db}|$ and $|\lambda^{t'}_{sb}|$ which is similar to the correlation between P and Q (upper-left panel Fig. 2) as expected since the slope of the curve is given by $\frac{Q}{P\lambda}$. In the upper-right panel of Fig. 3 we show the correlation between $|\lambda^{t'}_{db}|$ and $|\lambda^{b'}_{uc}|$ and note that $|\lambda^{b'}_{uc}|$ could be as large as 0.0025 when $|\lambda^{t'}_{db}|$ is very small (say $<$0.0005) i.e., when $P \ll Q$ and vice versa. The most interesting one is the correlation between $|\lambda^{t'}_{sb}|$ and $|\lambda^{b'}_{uc}|$ (lower-panel Fig. 3); it shows an almost linear relationship between them which is prominent for larger values of $|\lambda^{t'}_{sb}|$, i.e., for larger values of Q due to strong Q^2 dependence of $|\lambda^{b'}_{uc}|$. It plays an important role in understanding the correlations between the CP asymmetries in the B_s and D system; below we will discuss it in detail. The final remark from these discussions is that the allowed parameter space for the new CKM4 parameter space is highly correlated; random choices of the

TABLE IV. Allowed ranges of different CP observables related to B_d, B_s, and D^0 systems in SM3 and SM4; current experimental status is also given.

CP observable	SM3	Exp	SM4 ranges
$S_{\psi K_s} = \sin 2\beta_d$	0.739 ± 0.049	0.67 ± 0.02	$0.40 \rightarrow 0.90$
$S_{\psi\phi} = \sin\phi_s^{\psi\phi}$	-0.04 ± 0.002	$[-0.04, -0.86]$ CDF	$-0.60 \rightarrow 0.60$
		$[-0.37, -0.90]$ DO	
$a_{\rm sl}^d$	$(-4.8^{+1.0}_{-1.2}) \times 10^{-4}$	-0.0047 ± 0.0046	> -0.002
$a_{\rm sl}^s$	$(2.1 \pm 0.6) \times 10^{-5}$	-0.0146 ± 0.0075	$-0.005 \rightarrow 0.005$ (Eq. (30))
$\eta_f S_{CP}(D)$	$\approx -2 \times 10^{-6}$	$-0.248 \pm 0.496\%$	$-0.01 \rightarrow 0.01$
$a_{\rm sl}(D)$	$\approx 1 \times 10^{-4}$		$-0.6 \rightarrow 0.6$

CKM4 parameters should not be done, in fact chosen values should be consistent with the appropriate correlations.

Let us move to next part of our discussion where we show the effect of the fourth generation on different observables related to the B_d, B_s, and D system. As mentioned previously SM4 is quite different from most extensions of the SM in the sense that it is highly constrained. This motivates us to search for observables that can be used to confirm or rule out SM4. With this in mind we study the CP asymmetries $S_{\psi K_s}$, $a_{\rm sl}^d$, $S_{\psi\phi}$, and $a_{\rm sl}^s$ and correlations among them.

In Fig. 4 (upper-left panel) we show CP asymmetry $S_{\psi K_s}$ as a function of $\lambda_{db}^{t'}$ and note that $S_{\psi K_s}$ can go down to ≈ 0.4 or can reach around 0.9 for large values of the product coupling $|\lambda_{db}^{t'}|$; so agreement with or appreciable deviation from the present experimental measurement are, in principle, both possible. We do not get any noticeable correlation between $S_{\psi K_s}$ with the phase $\delta_{t'd}$ of $\lambda_{db}^{t'}$. Finally, we note that though SM4 allows $|\Delta_d|$ to have values within the range $0.65 \lesssim |\Delta_d| \lesssim 1.25$ [Eq. (7)], it does not have any noticeable correlation with $S_{\psi K_s}$. In the upper-right panel of Fig. 4 we show the semileptonic asymmetry $a_{\rm sl}^d$ [Eqs. (5) and (8)] as a function of $S_{\psi K_s}$. We see that while, in principle, in SM4, $-0.002 \lesssim a_{\rm sl}^d \lesssim 0.002$, the experimental bound on $S_{\psi K_s}$ allows only $a_{\rm sl}^d \gtrsim -0.001$. Recall that SM has a bound, $(-4.8^{+1.0}_{-1.2}) \times 10^{-4}$ as shown by the black band in the Fig. 4 (upper-right panel). Thus, in SM4, $a_{\rm sl}^d$ can be large by a factor of about 2 or 3; even more importantly the correlation between $a_{\rm sl}^d$ and $S_{\psi K_s}$ can be very useful for testing the SM4.

Similarly, in the lower-left panel of Fig. 4 we are showing the allowed regions for the CP asymmetry $S_{\psi\phi}$ in $B_s \rightarrow \psi\phi$ as a function of $|\lambda_{sb}^{t'}|$, for 375 GeV $< m_{t'} <$ 575 GeV, $S_{\psi\phi}$ is bounded by $-0.60 < S_{\psi\phi} < 0.60$,[4] the explicit dependence on $m_{t'}$ has been shown in our earlier papers [13,14]. It is also interesting to note that its magnitude increases with $|\lambda_{sb}^{t'}|$; precise measurements of $S_{\psi\phi}$ will be helpful to put tighter constraints on $|\lambda_{sb}^{t'}|$ and the corresponding phase. Recently CDF and D0 have updated their measurement of the CP-violating phase with a data sample corresponding to an integrated luminosity of 5.2 fb^{-1} and 6.1 fb^{-1}, respectively. The allowed 68% C.L. ranges are [60,61]

$$\begin{aligned} \phi_s^{\psi\phi} &\in [-0.04, -1.04] \cup [-2.16, -3.10] \quad \text{CDF}, \\ &\in -0.76^{+0.38}_{-0.36}(\text{stat}) \pm 0.02(\text{syst}) \quad \text{D0}. \end{aligned} \tag{29}$$

[4] Actually the limit is $|S_{\psi\phi}| \lesssim 0.56$, it is rounded up to 0.6.

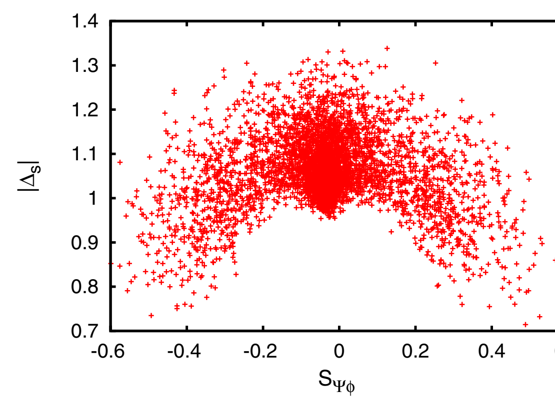

FIG. 5 (color online). The correlation between $S_{\psi\phi}$ and $|\Delta_s|$ [Eq. (7)] is shown.

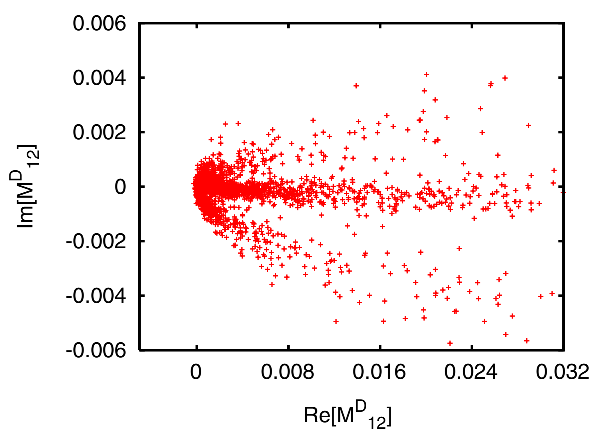

FIG. 6 (color online). The correlation between the real and imaginary part of the SD contribution to M_{12}^D is shown.

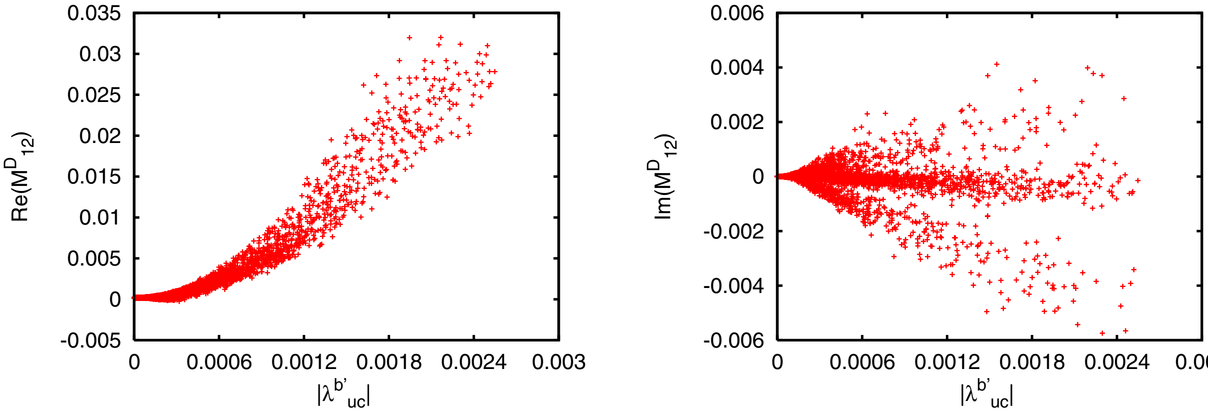

FIG. 7 (color online). Real (left panel) and imaginary (right panel) parts of the SD contribution to M_{12}^D as a function $|\lambda_{uc}^{b'}|$ are shown.

The corresponding 1σ ranges for $S_{\psi\phi} = \sin\phi_s^{\psi\phi}$ are given in Table IV.

In the lower-right panel of Fig. 4 we show the correlation[5] between $S_{\psi\phi}$ and $a_{\rm sl}^s$ [Eq. (5)] with $\frac{|\Gamma_{12}^s|}{|M_{12}^{s,\rm SM}|}$ [Eq. (8)] taken at 1σ (red) and 2σ (blue) of the theory error. We note that its magnitude increases with $S_{\psi\phi}$ as well as with the ratio $\frac{|\Gamma_{12}^s|}{|M_{12}^{s,\rm SM}|}$, as expected from Eq. (5). It is also important to note that $a_{\rm sl}^s$ is inversely proportional to $|\Delta_s|$. As shown in Fig. 5, $|\Delta_s|$ has a strong correlation with $S_{\psi\phi}$, we note that the values like $|\Delta_s| \approx 0.7$ are allowed for larger values of $|S_{\psi\phi}|$. Therefore, $a_{\rm sl}^s$ is expected to get an additional boost for lower values of $|\Delta_s|$ when $|S_{\psi\phi}|$ reaches its maximum value (≈ 0.5). The maximum allowed ranges in SM4 are thus given by

$$|a_{\rm sl}^s| \lesssim 0.004, \quad \frac{|\Gamma_{12}^s|}{|M_{12}^{s,\rm SM}|}@1\sigma, \quad \lesssim 0.005, \quad \frac{|\Gamma_{12}^s|}{|M_{12}^{s,\rm SM}|}@2\sigma. \tag{30}$$

Perhaps by taking the theory error on $\frac{|\Gamma_{12}^s|}{|M_{12}^{s,\rm SM}|}$ at 2σ we are exhibiting overabundance of caution. Be that as it may, it is clear that although SM4 can increase $a_{\rm sl}^s$ over SM3 by over 2 orders of magnitude, SM4 has difficulty actually reaching the central value of the D0 result. Given that the D0 results on $a_{\rm sl}^s$ is only $\sim 2\sigma$, and considering the fact that this is an extremely difficult measurement we do not believe at this point it is a concern for SM4. In our opinion the fragility of the experimental result suggests independent verification is essential.[6]

In Table IV we summarize the allowed ranges for different CP observables in SM4; it includes time-dependent CP asymmetries in $B_d \to \psi K_s$, $B_s \to \psi\phi$ as well as the semileptonic asymmetries associated with the B_d and B_s system [Eq. (5)]. We also mention the corresponding experimental ranges and SM3 predictions obtained with the inputs given in Table I.

In Fig. 6 we show the correlation between the real and imaginary parts of the SD contribution to $D^0 - \bar{D}^0$ mixing. Note that the magnitude of $\mathrm{Im}(M_{12}^D)$ could be as high as 0.6%, which could be negative or positive; very small number of points are allowed for $\mathrm{Re}(M_{12}^D) < 0$, however, it could be as high as 0.032. These findings are in good agreement with Ref. [16].

In Fig. 7 we plot real (left panel) and imaginary (right panel) parts of the SD contribution to M_{12}^D as a function of $|\lambda_{uc}^{b'}|$ and note that in both the cases its magnitude increases with the product coupling. In the case of the real part almost all the allowed points are for $\mathrm{Re}(M_{12}^D) > 0$, however, in case of imaginary part we have both positive and negative solutions. As noticed before (Fig. 3), $|\lambda_{sb}^{t'}|$ has a linear relationship with $|\lambda_{uc}^{b'}|$; a tighter constraint on $|\lambda_{sb}^{t'}|$, which is possible to get by reducing the errors in the measurements of B_d or B_s observables, will be helpful to put tighter constrain on $D^0 - \bar{D}^0$ mixing.

In Fig. 8 we plot the time-dependent CP asymmetry $\eta_f S_{CP}(D)$ [Eq. (23)] and the semileptonic asymmetry $a_{\rm sl}(D)$ [Eq. (25)] in the D system as a function of the phase of $\frac{q}{p}$ [Eq. (21)] and $|\frac{q}{p}|$, respectively; it could be directly compared with the correlations shown in [16]. We note that with the present experimental bound on the phase of $\frac{q}{p}$ [Eq. (26)], the magnitude of $\eta_f S_{CP}(D)$ could be enhanced up to the present experimental bound. On the other hand with the present constraint on $|\frac{q}{p}|$, $a_{\rm sl}(D)$ could be reduced to -0.6; again these results are also in agreement with Buras *et. al* [16].

In Fig. 9 we plot $S_{CP}(D)$ and $a_{\rm sl}(D)$ as a function of $|\lambda_{uc}^{b'}|$ and note that the magnitude of both may increase with $|\lambda_{uc}^{b'}|$; SM3 predictions and the allowed ranges in SM4 for the corresponding observables are summarized in Table IV.

[5]The plot corresponds to negative solution for $S_{\psi\phi}$, we do not show the points corresponding to the positive solution of $S_{\psi\phi}$ for which one should get a region symmetric to that shown in the figure.

[6]Lack of identification of B mesons is a very serious concern for this experimental result, see also footnote 1

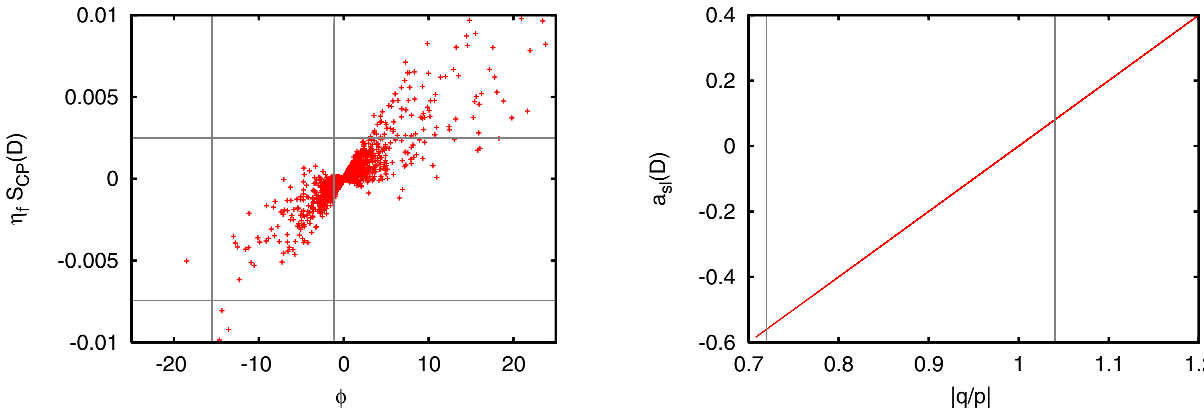

FIG. 8 (color online). Time-dependent CP asymmetry for the D system, $\eta_f S_{CP}(D)$, as a function of the phase ϕ of $\frac{q}{p}$ (left panel); semileptonic CP asymmetry, $a_{\rm sl}(D)$, as a function of $|\frac{q}{p}|$ (right panel). The corresponding SM value for $a_{\rm sl}(D)$ is $\mathcal{O}(10^{-4})$ [16]. The grey horizontal and vertical bands represent the corresponding experimental ranges.

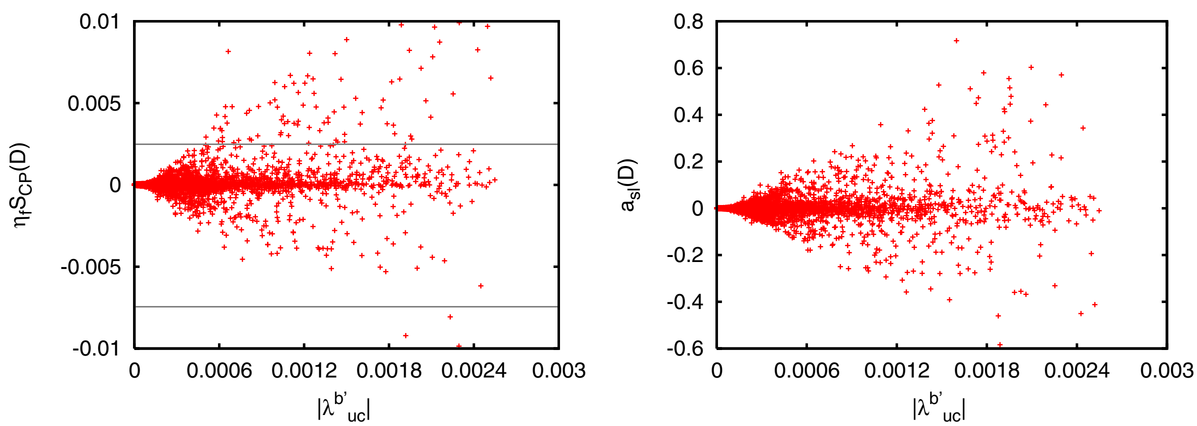

FIG. 9 (color online). $\eta_f S_{CP}(D)$ as a function of $|\lambda^{b'}_{uc}|$ (left panel) and $a_{\rm sl}(D)$ as a function $|\lambda^{b'}_{uc}|$ (right panel) are shown.

As discussed before (Fig. 4), the magnitude of $S_{\psi\phi}$ increases with the corresponding product coupling, we also noticed that $|\lambda^{b'}_{uc}|$ increases with $|\lambda^{t'}_{sb}|$ which indicates a definite correlation between $S_{\psi\phi}$ and $\eta_f S_{CP}(D)$ [16]. In the near future if we are able to put tighter constraints on $|\lambda^{t'}_{sb}|$, we will be able to get strong limit on $\eta_f S_{CP}(D)$ and $a_{\rm sl}(D)$ due to fourth generation effects.

III. CONCLUSION

This paper represents a continuation of our study of some of the properties of SM4, standard model with four generations. One feature of SM4 that distinguishes it from practically all other beyond the standard model scenarios is that it is highly constrained. Recognizing this, we have few objectives in mind for this work. First, we want to quantitatively ascertain how well SM4 is able to address a key anomaly for the standard model, i.e., $S_{\psi K_s}$. We also want to see how well SM4 can address the semileptonic asymmetries that have been much in the news recently. Simple intuitive arguments suggest that the CP asymmetries in $S_{\psi K_s}$ and $a^d_{\rm sl}$ should be strongly correlated and similarly, $S_{\psi\phi}$ and $a^s_{\rm sl}$.

Furthermore, we want to see how best experimental information can be used to extract the parameters of SM4 as efficiently and accurately as possible. With this in mind we are using a particular representation of the 4×4 mixing matrix which is specifically designed to be very effective in extracting information on the parameters of SM4 from B decays, supplemented by extending the hierarchical nature as for SM3, since many B-decay modes are highly sensitive to SM4. Of course, we understand that physics will not depend on which representation of 4×4 mixing matrix one uses. Recall, though, that even for the simpler case of the SM, a number of different representations have been studied over the past few decades.

Using the specific representation for the 4×4 mixing matrix mentioned above we obtain constraints and correlations on its elements using available data from K, B, and D decays as well as electroweak precision tests and oblique corrections and allowing the $m_{t'}$ mass to range from 375 to 575 GeV. Constraints obtained are then used to study the mixing induced and semileptonic CP asymmetries in B_d, B_s, and in D^0. Although SM4 allows $S(B_d \to \psi K_s)$ to be closer to experiment thus alleviating a key difficulty for SM3 that has been found in recent years and SM4 also allows $a_{\rm sl}^d$ to be bigger by a factor of $O(3)$, these two observables are strongly correlated. Thus, while $S_{\psi K_s}$ can be ≈ 0.70,[7] simultaneously SM4 restricts $|a_{\rm sl}^d| \lesssim 0.0015$. The B factories have a lot more data since they studied this asymmetry some years ago [10]; it would be very worthwhile to update this bound as it could provide a very useful nontrivial test of SM4.

In contrast to $a_{\rm sl}^d$, $a_{\rm sl}^s$ can be a lot bigger in SM4, and of opposite sign, than in SM3 where it is essentially negligible. Therefore, it would also be very useful to constrain this asymmetry as well as the linear combination $(A_{\rm sl}^b)$ [11] of the two. Interestingly, the large same sign dimuon asymmetry recently discovered by D0 [11] implies a rather large central value for $a_{\rm sl}^s$. This has the same sign as in SM4 though the central value of the D0 result is somewhat larger than the expected range in SM4; however, the significance of the D0 result is only about 2σ on $a_{\rm sl}^s$. We therefore do not believe it is wise to pay too much attention to the central value given the size of the experimental error ($\approx 50\%$). These asymmetries should be a high priority target for experiments at the Tevatron as well as at LHCb. In recent years Belle also has taken appreciable data at the $\Upsilon(5S)$ which should be used for placing bounds on these asymmetries. In the future, these asymmetries should also be a very useful target at the Super-B factories.

[7] $S_{\psi K_s}$ provides a clean measurement of $\sin 2\beta$ and it is well known that in SM the contamination due to QCD or electroweak penguins is small (less than a few percent [62]) in this decay. Although the effects are subdominant, SM4 can contribute to the decay $b \to c\bar{c}s$ through the penguin diagrams and the overall effects are expected to be below 5%. Because of the weak mass dependences of the Wilson coefficients the contributions from the QCD penguins ($P_{\rm QCD}^{\rm SM4}$) in SM4 are expected to be small compare to $P_{\rm QCD}^{\rm SM3}$ since there is an additional suppression of order λ^2 due to the CKM4 product coupling $\lambda_{bs}^{t'}$. Although the electroweak penguin ($P_{\rm EW}^{\rm SM4}$) in SM4 gets enhanced by $\approx 20\%$ with respect to $P_{\rm EW}^{\rm SM3}$ for heavy $m_{t'}$ ($\approx$500 GeV), its effect on $\sin 2\beta$ measurements are expected to be of similar size as that of $P_{\rm QCD}^{\rm SM}$.

ACKNOWLEDGMENTS

S. N. thanks the Theory Division of the Saha Institute of Nuclear Physics (SINP) for hospitality. S. N's work is financially supported by NSERC of Canada. The work of A. S. is supported in part by the U.S. DOE Grant No. DE-AC02-98CH10886(BNL).

Note Added.—Very recently Ref. [63] presented constraints on SM4 using a completely different representation of the 4×4 mixing matrix [64].

[1] E. Lunghi and A. Soni, Phys. Lett. B **666**, 162 (2008).
[2] E. Lunghi and A. Soni, J. High Energy Phys. 08 (2009) 051.
[3] A. Lenz *et al.* (CKMfitter Group), Phys. Rev. D **83**, 036004 (2011).
[4] M. Bona *et al.* (UTfit Collaboration), Phys. Lett. B **687**, 61 (2010).
[5] E. Lunghi and A. Soni, Phys. Rev. Lett. **104**, 251802 (2010).
[6] E. Lunghi and A. Soni, Phys. Lett. B **697**, 323 (2011).
[7] K. Nakamura *et al.* (Particle Data Group), J. Phys. G **37**, 075021 (2010).
[8] see, for example, M. Gronau and J. L. Rosner, Phys. Lett. B **644**, 237 (2007); H. Y. Cheng and C. K. Chua, Phys. Rev. D **80**, 114008 (2009).
[9] T. Aaltonen *et al.* (CDF Collaboration), Phys. Rev. Lett. **100**, 161802 (2008); arXiv:0712.2397; V. M. Abazov *et al.* (D0 Collaboration), Phys. Rev. Lett. **101**, 241801 (2008).
[10] D. Asner *et al.* (The Heavy Flavor Averaging Group), arXiv:1010.1589.
[11] V. M. Abazov *et al.* (D0 Collaboration), Phys. Rev. D **82**, 032001 (2010).
[12] V. M. Abazov *et al.* (D0 Collaboration), Phys. Rev. Lett. **105**, 081801 (2010).
[13] A. Soni, A. K. Alok, A. Gird, R. Mohanta, and S. Nandi, Phys. Lett. B **683**, 302 (2010).
[14] A. Soni, A. K. Alok, A. Giri, R. Mohanta, and S. Nandi, Phys. Rev. D **82**, 033009 (2010).
[15] A. J. Buras, B. Duling, T. Feldmann, T. Heidsieck, C. Promberger, and S. Recksiegel, J. High Energy Phys. 09 (2010) 106.
[16] A. J. Buras, B. Duling, T. Feldmann, T. Heidsieck, C. Promberger, and S. Recksiegel, J. High Energy Phys. 07 (2010) 094.
[17] W. S. Hou and C. Y. Ma, Phys. Rev. D **82**, 036002 (2010).
[18] See also M. Bobrowski, A. Lenz, J. Riedl, and J. Rohrwild, Phys. Rev. D **79**, 113006 (2009); O. Eberhardt, A. Lenz, and J. Rohrwild, Phys. Rev. D **82**, 095006 (2010).
[19] W. S. Hou, Chin. J. Phys. (Taipei) **47**, 134 (2009).
[20] For earlier related works see C. Jarlskog and R. Stora, Phys. Lett. B **208**, 268 (1988); F. del Aguila and J. A. Aguilar-Saavedra, Phys. Lett. B **386**, 241 (1996); F. del Aguila, J. A. Aguilar-Saavedra, and G. C. Branco, Nucl. Phys. **B510**, 39 (1998).
[21] J. Carpenter, R. Norton, S. Siegemund-Broka, and A. Soni, Phys. Rev. Lett. **65**, 153 (1990). In passing, we note that the quark mass needed for dynamical electroweak symmetry breaking in this work, translated to the fourth family quasi-degenerate doublet, gives $m_{t'} \sim 500$ GeV and $m_H \approx \sqrt{2} m_{t'} \sim 700$ GeV.
[22] See the *Proceedings of the First International Symposium on the fourth family of quarks and leptons, Santa Monica,*

CA, 1987, edited by D. Cline and A. Soni (NY Academy of Sciences, New York, 1987); see also the *Proceedings of the Second International Symposium on the fourth family of quarks and leptons, Santa Monica, CA, 1989* edited by D. Cline and A. Soni (NY Academy of Sciences, New York, 1989).

[23] B. Holdom, Phys. Rev. Lett. **57**, 2496 (1986); **58**, 177(E) (1987); W. A. Bardeen, C. T. Hill, and M. Lindner, Phys. Rev. D **41**, 1647 (1990); C. T. Hill, M. A. Luty, and E. A. Paschos, Phys. Rev. D **43**, 3011 (1991); P. Q. Hung and G. Isidori, Phys. Lett. B **402**, 122 (1997).

[24] P. Q. Hung and C. Xiong, Phys. Lett. B **694**, 430 (2011).

[25] M. Hashimoto and V. A. Miransky, Phys. Rev. D **81**, 055014 (2010).

[26] M. S. Chanowitz, Phys. Rev. D **79**, 113008 (2009).

[27] M. S. Chanowitz, Phys. Rev. D **82**, 035018 (2010).

[28] W. S. Hou, A. Soni, and H. Steger, Phys. Lett. B **192**, 441 (1987).

[29] L. Wolfenstein, Phys. Rev. Lett. **51**, 1945 (1983).

[30] W. S. Hou, R. S. Willey, and A. Soni, Phys. Rev. Lett. **58**, 1608 (1987); **60**, 2337(E) (1988).

[31] W. S. Hou, A. Soni, and H. Steger, Phys. Rev. Lett. **59**, 1521 (1987).

[32] A. Lenz and U. Nierste, J. High Energy Phys. 06 (2007) 072.

[33] R. Louvot *et al.* (Belle Collaboration), Phys. Rev. Lett. **102**, 021801 (2009); A. Drutskoy, arXiv:hep-ex/0605110.

[34] Ulrich Uwer, Flavor Physics in the LHC Era, November 8–12 2010, Singapore, http://www.ntu.edu.sg/ias/upcomingevents/FlavorPhysics/Pages/default.aspx.

[35] D. J. Antonio *et al.* (RBC Collaboration and UKQCD Collaboration), Phys. Rev. Lett. **100**, 032001 (2008); C. Kelly, Lattice 2010, June 14–19 2010, Sardinia, Italy, http://www.infn.it/Lattice2010; Y. Aoki *et al.*, arXiv:1012.4178.

[36] T. Bae *et al.*, Phys. Rev. D **82**, 114509 (2010).

[37] C. Aubin, J. Laiho, and R. S. Van de Water, Phys. Rev. D **81**, 014507 (2010).

[38] E. Gamiz, C. T. H. Davies, G. P. Lepage, J. Shigemitsu, and M. Wingate (HPQCD Collaboration), Phys. Rev. D **80**, 014503 (2009).

[39] E. Gamiz (private communication).

[40] S. Herrlich and U. Nierste, Nucl. Phys. **B419**, 292 (1994).

[41] A. J. Buras, M. Jamin, and P. H. Weisz, Nucl. Phys. **B347**, 491 (1990).

[42] S. Herrlich and U. Nierste, Phys. Rev. D **52**, 6505 (1995).

[43] A. J. Buras, D. Guadagnoli, and G. Isidori, Phys. Lett. B **688**, 309 (2010).

[44] CDF Collaboration, CDF note 10110, 2010, http://www-cdf.fnal.gov/physics/S10CDFResults.html.

[45] H. J. He, N. Polonsky, and S. f. Su, Phys. Rev. D **64**, 053004 (2001).

[46] V. A. Novikov, L. B. Okun, A. N. Rozanov, and M. I. Vysotsky, Phys. Lett. B **529**, 111 (2002).

[47] G. D. Kribs, T. Plehn, M. Spannowsky, and T. M. P. Tait, Phys. Rev. D **76**, 075016 (2007).

[48] J. Erler and P. Langacker, Phys. Rev. Lett. **105**, 031801 (2010).

[49] P. Q. Hung and M. Sher, Phys. Rev. D **77**, 037302 (2008).

[50] I. I. Bigi, M. Blanke, A. J. Buras, and S. Recksiegel, J. High Energy Phys. 07 (2009) 097.

[51] W. Altmannshofer, A. J. Buras, and P. Paradisi, Phys. Lett. B **688**, 202 (2010).

[52] E. Barberio *et al.* (Heavy Flavor Averaging Group Collaboration), averages of *b*-hadron properties at the end of 2006; updates available on http://www.slac.stanford.edu/xorg/hfag.

[53] E. Barberio *et al.* (Heavy Flavor Averaging Group Collaboration), averages of *b*-hadron and *c*-hadron properties at the end of 2007.

[54] A. J. Schwartz, arXiv:0911.1464.

[55] V. Lubicz and C. Tarantino, Nuovo Cimento Soc. Ital. Fis. B **123**, 674 (2008).

[56] J. Laiho, R. S. Van de Water, and E. Lunghi, arXiv:0910.2928.

[57] I. Allison *et al.* (HPQCD Collaboration), Phys. Rev. D **78**, 054513 (2008).

[58] C. W. Bernard, T. Draper, G. Hockney, and A. Soni, Phys. Rev. D **38**, 3540 (1988); R. Gupta, T. Bhattacharya, and S. R. Sharpe, Phys. Rev. D **55**, 4036 (1997); L. Lellouch and C. J. D. Lin (UKQCD Collaboration), Phys. Rev. D **64**, 094501 (2001); H. W. Lin, S. Ohta, A. Soni, and N. Yamada, Phys. Rev. D **74**, 114506 (2006). Although these results are obtained in the quenched approximation, we know now that for *B* parameters quenching effects are rather small; see Ref. [48].

[59] K. Blum, Y. Grossman, Y. Nir, and G. Perez, Phys. Rev. Lett. **102**, 211802 (2009).

[60] CDF collaboration, CDF note 10206, 2010, http://www-cdf.fnal.gov/physics/new/bottom/bottom.html.

[61] D0 Collaboration, Conference note 6098-CONF, 2010, www-d0.fnal.gov/Run2Physics/WWW/results/prelim/B/B60/.

[62] M. Ciuchini, M. Pierini, and L. Silvestrini, Phys. Rev. Lett. **95**, 221804 (2005); M. Gronau and J. L. Rosner, Phys. Lett. B **672**, 349 (2009).

[63] A. K. Alok, A. Dighe, and D. London, Phys. Rev. D **83**, 073008 (2011).

[64] C. S. Kim and A. S. Dighe, Int. J. Mod. Phys. E **16**, 1445 (2007).